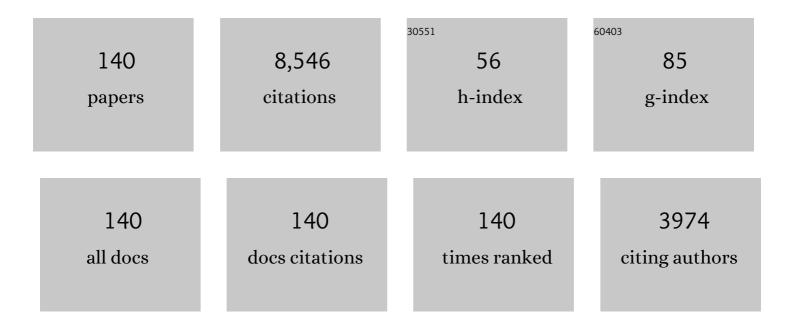
Ghasem Bahlakeh

List of Publications by Year in descending order

Source: https://exaly.com/author-pdf/9353910/publications.pdf Version: 2024-02-01



#	Article	IF	CITATIONS
1	Chitosan biomolecules-modified graphene oxide nano-layers decorated by mesoporous ZIF-9 nanocrystals for the construction of a smart/pH-triggered anti-corrosion coating system. Journal of Industrial and Engineering Chemistry, 2023, 121, 45-62.	2.9	3
2	Molecular-dynamic/DFT-electronic theoretical studies coupled with electrochemical investigations of the carrot pomace extract molecules inhibiting potency toward mild steel corrosion in 1AM HCl solution. Journal of Molecular Liquids, 2022, 346, 118344.	2.3	27
3	Multi-walled CNT decoration by ZIF-8 nanoparticles: O-MWCNT@ZIF-8/epoxy interfacial, thermal–mechanical properties analysis via combined DFT-D computational/experimental approaches. Journal of Industrial and Engineering Chemistry, 2022, 108, 170-187.	2.9	8
4	Chemically controlled nitrogen-doped reduced-Graphene/Graphite oxide frameworks for aiding superior thermal/anti-corrosion performance: Integrated DFT-D & experimental evaluations. Chemical Engineering Journal, 2022, 437, 135241.	6.6	17
5	Ultrastable Porous Covalent Organic Framework Assembled Carbon Nanotube as a Novel Nanocontainer for Anti-Corrosion Coatings: Experimental and Computational Studies. ACS Applied Materials & Interfaces, 2022, 14, 19958-19974.	4.0	32
6	Electronic DFT-D modeling of L-citrulline molecules interactions with Beta-CD aligned rGO-APTES multi-functional nano-capsule for anti-corrosion application. Journal of Molecular Liquids, 2022, 354, 118814.	2.3	9
7	Metal-doped 2D rGO nano-sheets fabrication utilizing plant source bio-molecules and application in the epoxy anti-corrosive coating: Combined experimental and DFT-D modeling investigations. Progress in Organic Coatings, 2022, 170, 106938.	1.9	5
8	Flow injection chemiluminescence determination of ethion and computational investigation of the adsorption process on molecularly imprinted polymerized high internal phase emulsion. Luminescence, 2022, 37, 1514-1523.	1.5	1
9	Synthesis of graphene oxide nanosheets decorated by nanoporous zeolite-imidazole (ZIF-67) based metal-organic framework with controlled-release corrosion inhibitor performance: Experimental and detailed DFT-D theoretical explorations. Journal of Hazardous Materials, 2021, 404, 124068.	6.5	114
10	Construction of an epoxy composite coating with exceptional thermo-mechanical properties using Zr-based NH2-UiO-66 metal-organic framework (MOF): Experimental and DFT-D theoretical explorations. Chemical Engineering Journal, 2021, 408, 127366.	6.6	62
11	Synthesis of a multi-functional zinc-centered nitrogen-rich graphene-like thin film from natural sources on the steel surface for achieving superior anti-corrosion properties. Corrosion Science, 2021, 178, 109077.	3.0	35
12	Development of an active/barrier bi-functional anti-corrosion system based on the epoxy nanocomposite loaded with highly-coordinated functionalized zirconium-based nanoporous metal-organic framework (Zr-MOF). Chemical Engineering Journal, 2021, 408, 127361.	6.6	89
13	Anti-corrosion performance of the mild steel substrate treated by a novel nanostructure europium oxide-based conversion coating: Electrochemical and surface studies. Colloids and Surfaces A: Physicochemical and Engineering Aspects, 2021, 609, 125689.	2.3	14
14	Application of nanoporous cobalt-based ZIF-67 metal-organic framework (MOF) for construction of an epoxy-composite coating with superior anti-corrosion properties. Corrosion Science, 2021, 178, 109099.	3.0	98
15	Construction of a high-potency anti-corrosive metal-organic film based on europium (III)-benzimidazole: Theoretical and electrochemical investigations. Construction and Building Materials, 2021, 269, 121271.	3.2	20
16	The role of ethanolic extract of Stachys byzantina's leaves for effective decreasing the mild-steel (MS) degradation in the acidic solution; coupled theoretical/experimental assessments. Journal of Molecular Liquids, 2021, 329, 115571.	2.3	30
17	MIL-88A (Fe) filler with duplicate corrosion inhibitive/barrier effect for epoxy coatings: Electrochemical, molecular simulation, and cathodic delamination studies. Journal of Industrial and Engineering Chemistry, 2021, 97, 200-215.	2.9	45
18	Superior inhibition action of the Mish Gush (MG) leaves extract toward mild steel corrosion in HCl solution: Theoretical and electrochemical studies. Journal of Molecular Liquids, 2021, 332, 115876.	2.3	86

#	Article	IF	CITATIONS
19	A comprehensive electronic-scale DFT modeling, atomic-level MC/MD simulation, and electrochemical/surface exploration of active nature-inspired phytochemicals based on Heracleum persicum seeds phytoextract for effective retardation of the acidic-induced corrosion of mild steel. Journal of Molecular Liquids, 2021, 331, 115764.	2.3	34
20	Theoretical and experimental assessment of a green corrosion inhibitor extracted from Malva sylvestris. Journal of Environmental Chemical Engineering, 2021, 9, 105256.	3.3	47
21	Superior thermal-mechanical properties of the epoxy composite reinforced with rGO-ATMP; Combined DFT-D theoretical modeling/experimental studies. Journal of Molecular Liquids, 2021, 331, 115800.	2.3	13
22	Increasing inhibition performance of simultaneous precipitation of calcium and strontium sulfate scales using a new inhibitor — Laboratory and field application. Journal of Petroleum Science and Engineering, 2021, 202, 108589.	2.1	19
23	Eco-friendly protocol for zinc-doped amorphous carbon-based film construction over steel surface using nature-inspired phytochemicals: Coupled experimental and classical atomic/molecular and electronic-level theoretical explorations. Journal of Environmental Chemical Engineering, 2021, 9, 105487	3.3	19
24	Improvement of the anti-corrosion ability of a silane film with β-cyclodextrin-based nanocontainer loaded with L-histidine: Coupled experimental and simulations studies. Progress in Organic Coatings, 2021, 157, 106288.	1.9	10
25	Detailed theoretical DFT computation/molecular simulation and electrochemical explorations of Thymus vulgaris leave extract for effective mild-steel corrosion retardation in HCl solution. Journal of Molecular Liquids, 2021, 335, 115897.	2.3	32
26	Cyclodextrin-based nano-carrier for intelligent delivery of dopamine in a self-healable anti-corrosion coating. Journal of Environmental Chemical Engineering, 2021, 9, 105457.	3.3	16
27	Fabrication of MIL-88A sandwiched in graphene oxide nanocomposites using a green approach to induce active/barrier protective functioning in epoxy coatings. Journal of Cleaner Production, 2021, 321, 128928.	4.6	27
28	Nano-scale P, Zn-codoped reduced-graphene oxide incorporated epoxy composite; synthesis, electronic-level DFT-D modeling, and anti-corrosion properties. Progress in Organic Coatings, 2021, 159, 106416.	1.9	17
29	Combined atomic-scale/DFT-theoretical simulations & electrochemical assessments of the chamomile flower extract as a green corrosion inhibitor for mild steel in HCl solution. Journal of Molecular Liquids, 2021, 342, 117570.	2.3	73
30	S, P-codoped rGO-phytic acid-polythiophene core–shell; synthesis, modeling, and dual active–passive anti-corrosion performance of epoxy nanocomposite. Journal of Industrial and Engineering Chemistry, 2021, 103, 102-117.	2.9	15
31	Benzimidazole loaded β-cyclodextrin as a novel anti-corrosion system; coupled experimental/computational assessments. Journal of Colloid and Interface Science, 2021, 603, 716-727.	5.0	32
32	Application of L-citrulline loaded beta-cyclodextrin nano-carrier for fabrication of a corrosion protective silane film on mild-steel. Progress in Organic Coatings, 2021, 161, 106484.	1.9	5
33	2D reduced-graphene oxide (rGO) nanosheets decorated with l-histidine loaded-β-cyclodextrin for efficient epoxy nano-composite anti-corrosion properties; DFT-D modeling/experimental assessments. FlatChem, 2021, 30, 100309.	2.8	18
34	Graphene oxide nanoplatform surface decoration by spherical zinc-polypyrrole nanoparticles for epoxy coating properties enhancement: Detailed explorations from integrated experimental and electronic-scale quantum mechanics approaches. Journal of Alloys and Compounds, 2020, 816, 152510.	2.8	27
35	Production of an environmentally stable anti-corrosion film based on Esfand seed extract molecules-metal cations: Integrated experimental and computer modeling approaches. Journal of Hazardous Materials, 2020, 382, 121029.	6.5	98
36	Integrated modeling and electrochemical study of Myrobalan extract for mild steel corrosion retardation in acidizing media. Journal of Molecular Liquids, 2020, 298, 112046.	2.3	59

#	Article	IF	CITATIONS
37	Fabrication of metal-organic based complex film based on three-valent samarium ions-[bis (phosphonomethyl) amino] methylphosphonic acid (ATMP) for effective corrosion inhibition of mild steel in simulated seawater. Construction and Building Materials, 2020, 239, 117812.	3.2	44
38	Experimental complemented with microscopic (electronic/atomic)-level modeling explorations of Laurus nobilis extract as green inhibitor for carbon steel in acidic solution. Journal of Industrial and Engineering Chemistry, 2020, 84, 52-71.	2.9	59
39	A detailed investigation of the chloride-induced corrosion of mild steel in the presence of combined green organic molecules of Primrose flower and zinc cations. Journal of Molecular Liquids, 2020, 297, 111862.	2.3	33
40	Rational assembly of mussel-inspired polydopamine (PDA)-Zn (II) complex nanospheres on graphene oxide framework tailored for robust self-healing anti-corrosion coatings application. Chemical Engineering Journal, 2020, 391, 123630.	6.6	113
41	Applying detailed molecular/atomic level simulation studies and electrochemical explorations of the green inhibiting molecules adsorption at the interface of the acid solution-steel substrate. Journal of Molecular Liquids, 2020, 299, 112220.	2.3	25
42	Construction of an epoxy composite with excellent thermal/mechanical properties using graphene oxide nanosheets reduced/functionalized by Tamarindus indiaca extract/zinc ions; detailed experimental and DFT-D computer modeling explorations. Results in Physics, 2020, 19, 103400.	2.0	12
43	Green synthesis of reduced graphene oxide nanosheets decorated with zinc-centered metal-organic film for epoxy-ester composite coating reinforcement: DFT-D modeling and experimental explorations. Journal of the Taiwan Institute of Chemical Engineers, 2020, 114, 311-330.	2.7	16
44	Fabrication of a novel hydrophobic anti-corrosion film based on Eu2O3/stearic acid on steel surface; Experimental and detailed computer modeling studies. Journal of the Taiwan Institute of Chemical Engineers, 2020, 114, 228-240.	2.7	3
45	A detailed study on the synergistic corrosion inhibition impact of the Quercetin molecules and trivalent europium salt on mild steel; electrochemical/surface studies, DFT modeling, and MC/MD computer simulation. Journal of Molecular Liquids, 2020, 316, 113914.	2.3	62
46	Detailed atomic/molecular-level/electronic-scale computer modeling and electrochemical explorations of the adsorption and anti-corrosion effectiveness of the green nitrogen-based phytochemicals on the mild steel surface in the saline solution. Journal of Molecular Liquids, 2020, 319, 114312.	2.3	16
47	Unique 2-methylimidazole based Inorganic Building Brick nano-particles (NPs) functionalized with 3-aminopropyltriethoxysilane with excellent controlled corrosion inhibitors delivery performance; Experimental coupled with molecular/DFT-D simulations. Journal of the Taiwan Institute of Chemical Engineers, 2020, 117, 209-222.	2.7	27
48	Theoretical MD/DFT computer explorations and surface-electrochemical investigations of the zinc/iron metal cations interactions with highly active molecules from Lemon balm extract toward the steel corrosion retardation in saline solution. Journal of Molecular Liquids, 2020, 310, 113220.	2.3	21
49	Construction of a unique anti-corrosion nanocomposite based on graphene oxide@Zn3PO4/epoxy; experimental characterization and detailed-theoretical quantum mechanics (QM) investigations. Construction and Building Materials, 2020, 256, 119439.	3.2	20
50	Synthesis of a non-hazardous/smart anti-corrosion nano-carrier based on beta-cyclodextrin-zinc acetylacetonate inclusion complex decorated graphene oxide (β-CD-ZnA-MGO). Journal of Hazardous Materials, 2020, 398, 122962.	6.5	36
51	Construction of a sustainable/controlled-release nano-container of non-toxic corrosion inhibitors for the water-based siliconized film: Estimating the host-guest interactions/desorption of inclusion complexes of cerium acetylacetonate (CeA) with beta-cyclodextrin (Î ² -CD) via detailed electronic/atomic-scale computer modeling and experimental methods. Journal of Hazardous	6.5	31
52	Materials, 2020, 399, 123046. Designing a novel targeted-release nano-container based on the silanized graphene oxide decorated with cerium acetylacetonate loaded beta-cyclodextrin (Î ² -CD-CeA-MGO) for epoxy anti-corrosion coating. Chemical Engineering Journal, 2020, 400, 125860.	6.6	63
53	Development and anti-corrosion performance of hyperbranched polyglycerol-decorated Fe3O4@SiO2 on mild steel in 1.0ÂM HCl. Journal of Molecular Liquids, 2020, 314, 113597.	2.3	15
54	Designing a non-hazardous nano-carrier based on graphene oxide@Polyaniline-Praseodymium (III) for fabrication of the Active/Passive anti-corrosion coating. Journal of Hazardous Materials, 2020, 398, 123136.	6.5	46

#	Article	IF	CITATIONS
55	Explorations of the adhesion and anti-corrosion properties of the epoxy coating on the carbon steel surface modified by Eu2O3 nanostructured film. Journal of Molecular Liquids, 2020, 314, 113658.	2.3	8
56	Corrosion prevention of AISI 304 stainless steel in hydrochloric acid medium using garlic extract as a green corrosion inhibitor: Electrochemical and theoretical studies. Journal of Molecular Liquids, 2020, 315, 113679.	2.3	70
57	Construction of a highly-effective/sustainable corrosion protective composite nanofilm based on Aminotris(methylphosphonic acid) and trivalent cerium ions on mild steel against chloride solution. Construction and Building Materials, 2020, 261, 119838.	3.2	19
58	Estimating the synergistic corrosion inhibition potency of (2-(3,4-)-3,5,7-trihydroxy-4H-chromen-4-one) and trivalent-cerium ions on mild steel in NaCl solution. Construction and Building Materials, 2020, 261, 119923.	3.2	29
59	Potential role of a novel green eco-friendly inhibitor in corrosion inhibition of mild steel in HCl solution: Detailed macro/micro-scale experimental and computational explorations. Construction and Building Materials, 2020, 245, 118464.	3.2	121
60	Probing molecular adsorption/interactions and anti-corrosion performance of poppy extract in acidic environments. Journal of Molecular Liquids, 2020, 304, 112750.	2.3	63
61	Development of metal-organic framework (MOF) decorated graphene oxide nanoplatforms for anti-corrosion epoxy coatings. Carbon, 2020, 161, 231-251.	5.4	260
62	A green assisted route for the fabrication of a high-efficiency self-healing anti-corrosion coating through graphene oxide nanoplatform reduction by Tamarindus indiaca extract. Journal of Hazardous Materials, 2020, 390, 122147.	6.5	83
63	Steel corrosion lowering in front of the saline solution by a nitrogen-rich source of green inhibitors: Detailed surface, electrochemical and computational studies. Construction and Building Materials, 2020, 254, 119266.	3.2	31
64	Aloysia citrodora leaves extract corrosion retardation effect on mild-steel in acidic solution: Molecular/atomic scales and electrochemical explorations. Journal of Molecular Liquids, 2020, 310, 113221.	2.3	39
65	Detailed-level computer modeling explorations complemented with comprehensive experimental studies of Quercetin as a highly effective inhibitor for acid-induced steel corrosion. Journal of Molecular Liquids, 2020, 309, 113035.	2.3	64
66	Graphene oxide nanoplatforms reduction by green plant-sourced organic compounds for construction of an active anti-corrosion coating; experimental/electronic-scale DFT-D modeling studies. Chemical Engineering Journal, 2020, 397, 125433.	6.6	57
67	Construction of a zinc-centered metal–organic film with high anti-corrosion potency through covalent-bonding between the natural flavonoid-based molecules (Quercetin)/divalent-zinc: Computer modeling (integrated-DFT&MC/MD)/electrochemical-surface assessments. Journal of Industrial and Engineering Chemistry, 2020, 88, 382-395.	2.9	20
68	Utilizing Lemon Balm extract as an effective green corrosion inhibitor for mild steel in 1M HCl solution: A detailed experimental, molecular dynamics, Monte Carlo and quantum mechanics study. Journal of the Taiwan Institute of Chemical Engineers, 2019, 95, 252-272.	2.7	242
69	Highly effective mild steel corrosion inhibition in 1â€⁻M HCl solution by novel green aqueous Mustard seed extract: Experimental, electronic-scale DFT and atomic-scale MC/MD explorations. Journal of Molecular Liquids, 2019, 293, 111559.	2.3	124
70	A detailed computational exploration and experimental surface/electrochemical analyses of mild steel functionalized by zinc-aminotris methylene phosphonic acid complex film. Applied Surface Science, 2019, 495, 143582.	3.1	33
71	Study of the synergistic effect of Mangifera indica leaves extract and zinc ions on the mild steel corrosion inhibition in simulated seawater: Computational and electrochemical studies. Journal of Molecular Liquids, 2019, 292, 111387.	2.3	97
72	Polyurethane coatings reinforced with 3-(triethoxysilyl)propyl isocyanate functionalized graphene oxide nanosheets: Mechanical and anti-corrosion properties. Progress in Organic Coatings, 2019, 136, 105243.	1.9	21

#	Article	IF	CITATIONS
73	Green Eucalyptus leaf extract: A potent source of bio-active corrosion inhibitors for mild steel. Bioelectrochemistry, 2019, 130, 107339.	2.4	124
74	A green complex film based on the extract of Persian Echium amoenum and zinc nitrate for mild steel protection in saline solution; Electrochemical and surface explorations besides dynamic simulation. Journal of Molecular Liquids, 2019, 291, 111281.	2.3	31
75	Photocatalytic, corrosion protection and adhesion properties of acrylic nanocomposite coating containing silane treated nano zinc oxide: A combined experimental and simulation study. Progress in Organic Coatings, 2019, 135, 496-509.	1.9	23
76	Molecular/electronic/atomic-level simulation and experimental exploration of the corrosion inhibiting molecules attraction at the steel/chloride-containing solution interface. Journal of Molecular Liquids, 2019, 296, 111809.	2.3	48
77	Combined molecular simulation, DFT computation and electrochemical studies of the mild steel corrosion protection against NaCl solution using aqueous Eucalyptus leaves extract molecules linked with zinc ions. Journal of Molecular Liquids, 2019, 294, 111550.	2.3	43
78	Electronic/atomic level fundamental theoretical evaluations combined with electrochemical/surface examinations of Tamarindus indiaca aqueous extract as a new green inhibitor for mild steel in acidic solution (HCl 1ÂM). Journal of the Taiwan Institute of Chemical Engineers, 2019, 102, 349-377.	2.7	93
79	Application of green molecules from Chicory aqueous extract for steel corrosion mitigation against chloride ions attack; the experimental examinations and electronic/atomic level computational studies. Journal of Molecular Liquids, 2019, 290, 111176.	2.3	79
80	Graphene oxide nano-sheets loading with praseodymium cations: Adsorption-desorption study, quantum mechanics calculations and dual active-barrier effect for smart coatings fabrication. Journal of Industrial and Engineering Chemistry, 2019, 78, 143-154.	2.9	37
81	Elucidating detailed experimental and fundamental understandings concerning the green organic-inorganic corrosion inhibiting molecules onto steel in chloride solution. Journal of Molecular Liquids, 2019, 290, 111212.	2.3	66
82	Eriobotrya japonica Lindl leaves extract application for effective corrosion mitigation of mild steel in HCl solution: Experimental and computational studies. Construction and Building Materials, 2019, 220, 161-176.	3.2	64
83	Adsorption mechanism and synergistic corrosion-inhibiting effect between the green Nettle leaves extract and Zn2+ cations on carbon steel. Journal of Industrial and Engineering Chemistry, 2019, 77, 323-343.	2.9	81
84	Detailed macro-/micro-scale exploration of the excellent active corrosion inhibition of a novel environmentally friendly green inhibitor for carbon steel in acidic environments. Journal of the Taiwan Institute of Chemical Engineers, 2019, 100, 239-261.	2.7	87
85	Novel cost-effective and high-performance green inhibitor based on aqueous Peganum harmala seed extract for mild steel corrosion in HCl solution: Detailed experimental and electronic/atomic level computational explorations. Journal of Molecular Liquids, 2019, 283, 174-195.	2.3	175
86	A detailed electrochemical/theoretical exploration of the aqueous Chinese gooseberry fruit shell extract as a green and cheap corrosion inhibitor for mild steel in acidic solution. Journal of Molecular Liquids, 2019, 282, 366-384.	2.3	176
87	Interfacial adhesion and corrosion protection properties improvement of a polyester-melamine coating by deposition of a novel green praseodymium oxide nanofilm: A comprehensive experimental and computational study. Journal of Industrial and Engineering Chemistry, 2019, 74, 26-40.	2.9	12
88	Green method of carbon steel effective corrosion mitigation in 1†M HCl medium protected by Primula vulgaris flower aqueous extract via experimental, atomic-level MC/MD simulation and electronic-level DFT theoretical elucidation. Journal of Molecular Liquids, 2019, 284, 658-674.	2.3	74
89	A detailed atomic level computational and electrochemical exploration of the Juglans regia green fruit shell extract as a sustainable and highly efficient green corrosion inhibitor for mild steel in 3.5â€~wt% NaCl solution. Journal of Molecular Liquids, 2019, 284, 682-699.	2.3	138
90	Development of a nanostructured Ce(III)-Pr(III) film for excellently corrosion resistance improvement of epoxy/polyamide coating on carbon steel. Journal of Alloys and Compounds, 2019, 792, 375-388.	2.8	26

#	Article	IF	CITATIONS
91	A combined experimental and theoretical study of green corrosion inhibition of mild steel in HCl solution by aqueous Citrullus lanatus fruit (CLF) extract. Journal of Molecular Liquids, 2019, 279, 603-624.	2.3	145
92	Use of Rosa canina fruit extract as a green corrosion inhibitor for mild steel in 1 M HCl solution: A complementary experimental, molecular dynamics and quantum mechanics investigation. Journal of Industrial and Engineering Chemistry, 2019, 69, 18-31.	2.9	209
93	Corrosion inhibition of mild steel in 1†MHCl solution by ethanolic extract of eco-friendly Mangifera indica (mango) leaves: Electrochemical, molecular dynamics, Monte Carlo and ab initio study. Applied Surface Science, 2019, 463, 1058-1077.	3.1	214
94	A combined electrochemical, molecular dynamics, quantum mechanics and XPS analysis of the mild steel surface protected by a complex film composed of neodymium (III) and benzimidazole. Applied Surface Science, 2019, 464, 178-194.	3.1	49
95	Graphene oxide as a pH-sensitive carrier for targeted delivery of eco-friendly corrosion inhibitors in chloride solution: Experimental and theroretical investigations. Journal of Industrial and Engineering Chemistry, 2019, 72, 196-213.	2.9	81
96	Development of a high-performance corrosion protective functional nano-film based on poly acrylic acid-neodymium nitrate on mild steel surface. Journal of the Taiwan Institute of Chemical Engineers, 2019, 96, 610-626.	2.7	29
97	The role of chrome and zinc free-based neodymium oxide nanofilm on adhesion and corrosion protection properties of polyester/melamine coating on mild steel: Experimental and molecular dynamics simulation study. Journal of Cleaner Production, 2019, 210, 872-886.	4.6	26
98	Potential of Borage flower aqueous extract as an environmentally sustainable corrosion inhibitor for acid corrosion of mild steel: Electrochemical and theoretical studies. Journal of Molecular Liquids, 2019, 277, 895-911.	2.3	199
99	Mild steel surface eco-friendly treatment by Neodymium-based nanofilm for fusion bonded epoxy coating anti-corrosion/adhesion properties enhancement in simulated seawater. Journal of Industrial and Engineering Chemistry, 2019, 72, 474-490.	2.9	27
100	In-situ synthesis of Zn doped polyaniline on graphene oxide for inhibition of mild steel corrosion in 3.5 wt.% chloride solution. Journal of Industrial and Engineering Chemistry, 2018, 63, 322-339.	2.9	94
101	The role of functionalized graphene oxide on the mechanical and anti-corrosion properties of polyurethane coating. Journal of the Taiwan Institute of Chemical Engineers, 2018, 86, 199-212.	2.7	106
102	Polyserotonin Nanoparticles as Multifunctional Materials for Biomedical Applications. ACS Nano, 2018, 12, 4761-4774.	7.3	57
103	Glycyrrhiza glabra leaves extract as a green corrosion inhibitor for mild steel in 1 M hydrochloric acid solution: Experimental, molecular dynamics, Monte Carlo and quantum mechanics study. Journal of Molecular Liquids, 2018, 255, 185-198.	2.3	346
104	Highly effective inhibition of mild steel corrosion in 3.5% NaCl solution by green Nettle leaves extract and synergistic effect of eco-friendly cerium nitrate additive: Experimental, MD simulation and QM investigations. Journal of Molecular Liquids, 2018, 256, 67-83.	2.3	173
105	New detailed insights on the role of a novel praseodymium nanofilm on the polymer/steel interfacial adhesion bonds in dry and wet conditions: An integrated molecular dynamics simulation and experimental study. Journal of the Taiwan Institute of Chemical Engineers, 2018, 85, 221-236.	2.7	33
106	Fabrication of an efficient system for Zn ions removal from industrial wastewater based on graphene oxide nanosheets decorated with highly crystalline polyaniline nanofibers (GO-PANI): Experimental and ab initio quantum mechanics approaches. Chemical Engineering Journal, 2018, 337, 385-397.	6.6	84
107	Polyaniline-cerium oxide (PAni-CeO 2) coated graphene oxide for enhancement of epoxy coating corrosion protection performance on mild steel. Corrosion Science, 2018, 137, 111-126.	3.0	273
108	Impact of size-controlled p-phenylenediamine (PPDA)-functionalized graphene oxide nanosheets on the GO-PPDA/Epoxy anti-corrosion, interfacial interactions and mechanical properties enhancement: Experimental and quantum mechanics investigations. Chemical Engineering Journal, 2018, 335, 737-755.	6.6	140

#	Article	IF	CITATIONS
109	Construction of a highly effective self-repair corrosion-resistant epoxy composite through impregnation of 1H-Benzimidazole corrosion inhibitor modified graphene oxide nanosheets (GO-BIM). Corrosion Science, 2018, 145, 119-134.	3.0	95
110	Studying the Urtica dioica leaves extract inhibition effect on the mild steel corrosion in 1 M HCl solution: Complementary experimental, ab initio quantum mechanics, Monte Carlo and molecular dynamics studies. Journal of Molecular Liquids, 2018, 272, 120-136.	2.3	74
111	A combined experimental and electronic-structure quantum mechanics approach for studying the kinetics and adsorption characteristics of zinc nitrate hexahydrate corrosion inhibitor on the graphene oxide nanosheets. Applied Surface Science, 2018, 462, 963-979.	3.1	50
112	Cerium oxide nanoparticles influences on the binding and corrosion protection characteristics of a melamine-cured polyester resin on mild steel: An experimental, density functional theory and molecular dynamics simulation study. Corrosion Science, 2017, 118, 69-83.	3.0	77
113	Experimental investigation and molecular dynamics simulation of acid-doped polybenzimidazole as a new membrane for air-breathing microbial fuel cells. Journal of Membrane Science, 2017, 535, 221-229.	4.1	19
114	Corrosion protection properties and interfacial adhesion mechanism of an epoxy/polyamide coating applied on the steel surface decorated with cerium oxide nanofilm: Complementary experimental, molecular dynamics (MD) and first principle quantum mechanics (QM) simulation methods. Applied Surface Science, 2017, 419, 650-669.	3.1	69
115	Complementary experimental and quantum mechanics approaches for exploring the mechanical characteristics of epoxy composites loaded with graphene oxide-polyaniline nanofibers. Journal of Industrial and Engineering Chemistry, 2017, 53, 348-359.	2.9	40
116	A Detailed Molecular Dynamics Simulation and Experimental Investigation on the Interfacial Bonding Mechanism of an Epoxy Adhesive on Carbon Steel Sheets Decorated with a Novel Cerium–Lanthanum Nanofilm. ACS Applied Materials & Interfaces, 2017, 9, 17536-17551.	4.0	85
117	Cure kinetics of epoxy/ β -cyclodextrin-functionalized Fe 3 O 4 nanocomposites: Experimental analysis, mathematical modeling, and molecular dynamics simulation. Progress in Organic Coatings, 2017, 110, 172-181.	1.9	62
118	Corrosion protective and adhesion properties of a melamine-cured polyester coating applied on steel substrate treated by a nanostructure cerium–lanthanum film. Journal of the Taiwan Institute of Chemical Engineers, 2017, 81, 419-434.	2.7	20
119	Fabrication of a Highly Tunable Graphene Oxide Composite through Layer-by-Layer Assembly of Highly Crystalline Polyaniline Nanofibers and Green Corrosion Inhibitors: Complementary Experimental and First-Principles Quantum-Mechanics Modeling Approaches. Journal of Physical Chemistry C, 2017, 121, 20433-20450.	1.5	92
120	Synthesis of graphene oxide nanosheets functionalized by green corrosion inhibitive compounds to fabricate a protective system. Corrosion Science, 2017, 127, 240-259.	3.0	116
121	Calorimetric analysis and molecular dynamics simulation of cure kinetics of epoxy/chitosan-modified Fe3O4 nanocomposites. Progress in Organic Coatings, 2017, 112, 176-186.	1.9	56
122	Active corrosion protection of mild steel by an epoxy ester coating reinforced with hybrid organic/inorganic green inhibitive pigment. Journal of Alloys and Compounds, 2017, 728, 1289-1304.	2.8	68
123	Experimental and theoretical studies of the synergistic inhibition effects between the plant leaves extract (PLE) and zinc salt (ZS) in corrosion control of carbon steel in chloride solution. Journal of Molecular Liquids, 2017, 248, 854-870.	2.3	117
124	<scp>M</scp> orphological and transport characteristics of swollen chitosanâ€based proton exchange membranes studied by molecular modeling. Biopolymers, 2017, 107, 5-19.	1.2	6
125	Exploring the hydrated microstructure and molecular mobility in blend polyelectrolyte membranes by quantum mechanics and molecular dynamics simulations. RSC Advances, 2016, 6, 35517-35526.	1.7	24
126	A Close-up of the Effect of Iron Oxide Type on the Interfacial Interaction between Epoxy and Carbon Steel: Combined Molecular Dynamics Simulations and Quantum Mechanics. Journal of Physical Chemistry C, 2016, 120, 11014-11026.	1.5	87

#	Article	IF	CITATIONS
127	Rheological Study and Molecular Dynamics Simulation of Biopolymer Blend Thermogels of Tunable Strength. Biomacromolecules, 2016, 17, 3474-3484.	2.6	18
128	Microfluidic Manipulation of Core/Shell Nanoparticles for Oral Delivery of Chemotherapeutics: A New Treatment Approach for Colorectal Cancer. Advanced Materials, 2016, 28, 4134-4141.	11.1	74
129	Enhanced osteogenic differentiation of stem cells via microfluidics synthesized nanoparticles. Nanomedicine: Nanotechnology, Biology, and Medicine, 2015, 11, 1809-1819.	1.7	49
130	On-chip synthesis of fine-tuned bone-seeking hybrid nanoparticles. Nanomedicine, 2015, 10, 3431-3449.	1.7	43
131	Air-breathing microbial fuel cell with enhanced performance using nanocomposite proton exchange membranes. Polymer, 2014, 55, 6102-6109.	1.8	18
132	Polyelectrolyte Nanocomposite Membranes, Based on Chitosan-phosphotungstic Acid Complex and Montmorillonite for Fuel Cells Applications. Journal of Macromolecular Science - Physics, 2013, 52, 1226-1241.	0.4	17
133	A microfluidic approach to synthesizing high-performance microfibers with tunable anhydrous proton conductivity. Lab on A Chip, 2013, 13, 4549.	3.1	17
134	Sulfonated Aromatic Polymers and Organically Modified Montmorillonite Nanocomposite Membranes for Fuel Cells Applications. Journal of Macromolecular Science - Physics, 2013, 52, 1578-1590.	0.4	14
135	Understanding structure and transport characteristics in hydrated sulfonated poly(ether ether) Tj ETQq1 1 0.784 Journal of Membrane Science, 2013, 429, 384-395.	314 rgBT / 4.1	Overlock 1 37
136	Investigation of the effects of methanol presence on characteristics of sulfonated aromatic electrolyte membranes: Molecular dynamics simulations. Journal of Power Sources, 2013, 243, 935-945.	4.0	22
137	Molecular dynamics simulation study of proton diffusion in polymer electrolyte membranes based on sulfonated poly (ether ether ketone). International Journal of Hydrogen Energy, 2012, 37, 10256-10264.	3.8	65
138	Molecular dynamics simulation analysis of hydration effects on microstructure and transport dynamics in sulfonated poly(2,6-dimethyl-1,4-phenylene oxide) fuel cell membranes. International Journal of Hydrogen Energy, 2012, 37, 12714-12724.	3.8	30
139	Direct methanol fuel cell performance of sulfonated poly (2,6-dimethyl-1,4-phenylene) Tj ETQq1 1 0.784314 rgBT Energy, 2011, 36, 3688-3696.	/Overlock 3.8	10 Tf 50 2(39
140	Combined clove extract bio-molecules and zinc(II) ion synergistic effects in steel corrosion mitigation in saline solution: electronic (DFT) modeling, atomic/molecular (MC/MD) simulations, and corrosion	2.9	5

measurement. Biomass Conversion and Biorefinery, 0, , .